Original article

Segmentation and Classification of Jaw Bone CT images using Curvelet based Texture features

Reddy T K[1], Kumaravel N [2]

Abstract

The evaluation of jaw bone trabecular structure and quality could be useful for characterization and response of the bone for dental implants. Current clinical methods for assessment of bone quality at the implant sites largely depend on assessing bone mineral density using Dual energy X-ray absorptionometry. However, this does not provide any information about bone structure which is considered to be an equally important factor in assessing bone quality. This paper presents a novel approach for computer analysis of trabecular (or cancellous) bone structure using multiresolution based texture analysis to evaluate changes taking place in the architecture of bone with age and gender. The findings are compared with Hounsfield Units measured from the CT machine at different sites, which is a standard reference. Fifty patients were subjected to clinical CT to obtain the CT number and texture based architectural parameters respectively. In each site texture features were extracted using gray level co-occurrence matrices (GLCM), Run length matrices, Histogram and curvelet based statistical & co occurrence analysis. A very difficult problem in classification techniques is the choice of features to distinguish between classes. However the performance of any classifier is not optimized when all features are used. The feature optimization problem is addressed using Principle component analysis in terms of the best recognition rate and the optimal number of features. Testing this on a series of 120 image sections of trabecular bone with normal, partial and total edentulous patients correctly classified over 90% of the porous bone group with an overall accuracy of 87.8%–95.2%.The results shows that by using the Classification & Regression Tree approach the combination of the features from gray level and Ist order statistics achieved overall classification accuracy in the range of 87.8-90.24%. Features selected from the curvelet based co occurrence matrix performed better with overall classification accuracy of 92.89%.In order to increase the success rate the classification is done using the combination of curvelet statistical features and curvelet co occurrence features as feature vector and using this, a mean success rate of 95.2% is obtained.

Keywords: Multiresolution analysis, Texture features, curvelets, Computed Tomography, Regression analysis, GLRLM.

Introduction

Since early times of implantation era preoperative studies includes incision of gingiva in order to get a view of the bone surface. Preoperative studies required because a jaw bone must offer proper quality and adequate quantity of the bone. The overall dental implant success rate is considered to be influenced by both the volume (quantity) and density (quality) of available bone for implant placement. Successful implants require good bone and plenty of it. The thickness of the bone and height of the jaw bone available is easily measured on CT scans. Quality of bone is one of the variables that, unfortunately, cannot be accurately determined prior to the placement of the implant. Bone quality, as described by Lekhom and Zarb [1], is of

1. T K Reddy, SKR Engineering College/ ECE, Anna University, Chennai, India
2. N Kumaravel, College of Engineering / ECE, Anna University, Chennai, India

For correspondence:

major importance for the success of an implant placement. For preoperative planning bone quality has been categorized into five classes that basically describe the relation of cortical and cancellous bone in a specified region of the jaw [Table 1]. The amount of cortical bone is responsible for the primary stability of the implant, where as cancellous bone is responsible for long term stability. Hence the characterization of cancellous bone architecture is of considerable interest to evaluate quality of the bone. At present, only the histomorphometry techniques [2] allows determination of cancellous bone architecture of a patient. However, it is an invasive technique, as a biopsy of around 1 cm in diameter is taken from the patient. As cancellous bone has anisotropic mechanical properties, textural parameters as related to trabeculae orientation may give clinically valuable information. The proposed method focuses on image based bone density classification that utilizes image gray scale values and multiresolution texture based image features. This work develops an algorithm that is able to support surgeon's decisions based on analysis of CT images of jaw bones. Dental CT is frequently used as a non-invasive in vivo measurement tool for cancellous bone density, the denser the bone, the higher amount of X-ray energy is attenuated, resulting in varying intensities in resultant CT data sets [3]. CT image inferred bone density and mechanical property relationships are important for osteoporosis research, computational modeling of patient specific bony anatomical structures, surgical planning and tissue engineering.

The micro architecture of open celled cancellous bone is highly anisotropic, and varies with age, medical condition and gender. This variance is present as density measurement which is based on the amount of bone tissue with in a cancellous bone specimen. In conjunction with bone density readings, a qualitative measurement of structural parameters may improve our ability to estimate bone strength in better way [4]. Frequency analysis obtains the image features relating to its structure which is useful in predicting bone properties. Multiresolution analysis allows for the preservation of an image according to certain levels of resolution or blurring. Broadly speaking, multiresolution analysis allow for the zooming in and out of the under lying texture structure. The wavelet based multiresolution analysis has been used in feature extraction since it has the ability of localization in both time domain and frequency domain, and can also focus in any detail of the object [5,6]. Therefore the texture extraction is not effected by the size of the pixel neighborhood. By decomposing the image into a series of high pass and low pass bands, the wavelet transform extracts directional details that capture horizontal, vertical and diagonal activity. However, these three linear, directions are limiting and might not capture enough directional information in noisy images, such as medical CT scans, which do not have strong horizontal, vertical and diagonal directional elements.

Ridgelets, like wavelets, provide multiresoltion texture information; however they capture structural information of an image, based on multiple radial directions in the frequency domain. The authors show in [7] that, the multi directional capabilities of the ridgelet transform provide better texture discrimination than its wavelet counter part. However, one of the limitations of this approach is the fact that ridgelets are most effective in detecting linear radial structures, which are also not dominant in medical images. A recent extension of ridgelet is the curvelet transform [8, 9]. Curvelets are proven to be particularly effective at detecting image activity along curves instead of radial directions. Curvelets also capture structural information along multiple scales, location and orientation. Instead of capturing

structural information along radial lines, the curvelet transform captures this structural activity along radial "wedges" in the frequency domain [10, 11]. In view of that, curvelet transform is firstly proposed to highlight the curved singularities in images for structure recognition.

Curvelet transform

Candes and Donoho in 2000 introduced the curvelet transform [8, 10-12]. The continuous curvelet transform can be defined by a pair of windows W(r) (a radial window) and V(t) (an angular window), with variables W as a frequency-domain variable, and r and θ as polar coordinates in the frequency-domain.

$$\sum_{j=-\infty}^{\infty} W^2(2^j r) = 1, \quad r \in (3/4, 3/2), \qquad (1)$$

$$\sum_{l=-\infty}^{\infty} V^2(t-l)) = 1, \quad t \in (-1/2, 1/2), \qquad (2)$$

A polar 'wedge' represented by U_j is supported by W and V, the radial and angular windows. U_j is defined in the Fourier domain by

$$U_j(r,\theta) = 2^{-3/4} W(2^{-j} r) V(2^{\lfloor j/2 \rfloor} \theta)/2\pi \qquad (3)$$

The curvelet transform can be defined as a function of x = (x1, x2) at scale 2^{-j} orientation θ_l, and position $x_k^{(j,l)}$ by

$$\Psi_{j,\,l,\,k}(x) = \psi_j (R_{\theta l}(x - x_k^{(j,l)})), \qquad (4)$$

where R_θ is the rotation in radians. Fig1 illustrates the polar 'wedges' represented by U_j. Further details are presented in [].

Texture analysis

Traditionally, texture features have been calculated using a variety of statistical, structural and spectral techniques including co-occurrence matrices [13], run length statistics [14], spectral measures, fractal dimensions, statistical moments, and multi resolution techniques such as wavelets [6], ridgelets [7] and curvelets [10,11]. Co-occurrence matrices are often used in texture analysis, since they are able to capture the spatial dependence of grey level values within an image. Common statistical measures used in texture analysis are mean, standard deviation, energy, entropy, contrast, homogeneity , variance, correlation, maximum probability, sum-mean, cluster tendency and inverse difference moment [15]. In this paper, the curvelet transform is applied on a 3D data set of DICOM images of 50 patients. Curvelet statistical features, such as mean and standard deviation obtained from the first level of sub bands and curvelet co-occurrence features are extracted from each of the curvelet sub bands from higher level wedges. The structural activity extracted from the curvelet transform of the image can be analyzed statistically to generate curvelet based statistical and co-occurrence texture features. Correlation coefficient is calculated to find the relationship between feature change and percentage calcium loss in different directions and to determine which features undergo changes most closely corresponding to bone mineral loss.

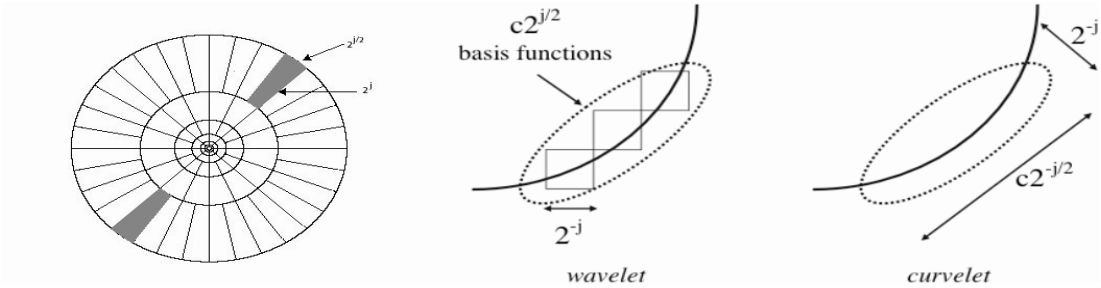

Figure 1: Curvelet tiling in the frequency domain [10].

Methodology

The algorithm proposed in this article consists of four main steps: Segmentation of regions of interest, application of the discrete curvelet transform, extraction of texture features, statistical analysis between HU and texture features based on gender and age and creation of a classifier. The following sections describe the data set, region of interest calculations, texture extraction methods and classifier performance.

Data set

From June 2006 to October 2008, 50 patient's age: 30 ~ 71 years with a mean of 50 years; 26 males and 24 females received the spiral CT examination. All patients needed dental implantations either in maxillae or mandible in selective locations. Single, partial, or total edentulous patients were included. Axial, panoramic and cross sectional images are acquired at each bone site with multi slice spiral CT scans (120 kv and 300 mAs, with a slice thickness of 0.625mm, pitch 0.4mm, scan time 750msi GE medical systems). The 3D DICOM image data consists of 190 consecutive 2D slices, each slice being 512x512 pixels in size and having 16 bit gray level resolution. The mean bone density of the implant recipient site was measured by using software incorporated in CT machine (GE). The bone density measurements were recorded in Hounsfield Units (HU). The scan was initially utilized to assess bone quality subjectively based on Lekholm and Zerb (1985) classification at anterior and posterior edentulous sites by rating the distribution of cortical and cancellous bone. Density of cancellous bone in Hounsfied units [HU] was determined by averaging the readings of multiple slices within respective sites. The classification of bone quality of each site and the CT analysis of cancellous bone densities are listed in Table1 and Table3. The density in HU for the cancellous bone sites varied widely, especially within the mandible, irrespective of the amount of cancellous bone. Curvelets like wavelets are extremely sensitive to contrast in the gray level intensity, the segmented images need further processing. In order to effectively use curvelet based texture descriptors, it is necessary to eliminate all background pixels to avoid mistaking the edge between the artificial background and the tissue as a texture feature. Each slice was therefore further cropped, and only square 32x32 sub- image fully contained in the interior of the segmented area are generated [see Fig 2 and Fig 3]. This size was chosen since the digital curvelet requires a 2n square image [9, 10].

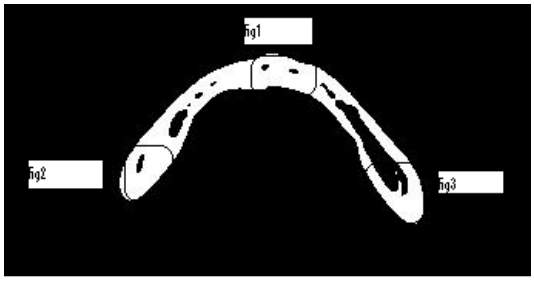

Figure 2: Segmented bone image with region of interest.

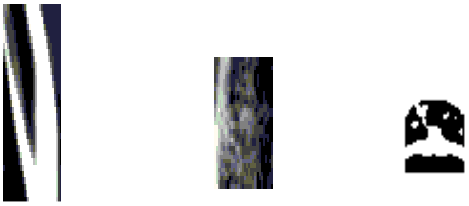

(Fig 3.1) (Fig 3.2) (Fig 3.3)

Fig 3: Region of interest [**Fig 3.1**-left posterior maxilla, **Fig 3.2**-right posterior maxilla, **Fig 3.3**-anterior maxilla.]

Feature extraction

Once the bone images were pre-processed the texture feature vectors used in the algorithm are derived from the Gray level run length matrix, image histogram and Discrete Curvelet Transform, introduced by Candes and Donono in [9]. Bone trabeculae appears in the image as an array of connected pixels having the same gray level range, which corresponds to the definition of a run. However, a 65,256

Table 1: Classification based on CT determination of Bone density [1]

Type of Bone	*CT value*	*Comments*
D1	>1250 HU	Homogeneous and compact bone.
D2	850-1250 HU	A thick layer of compact bone surrounding a core of dense trabecular bone
D3	350-850HU	A thin layer of cortical bone surrounding dense trabecular bone of favorable strength.
D4	150-350HU	A thin layer of cortical bone surrounding a core of low-density trabecular bone.
D5	<150 HU	Very soft bone with incomplete mineralization

level image (16 bit image slice) yields a huge number of runs having a small length which are not representative of the bone architecture, as the pixels in a trabecula do not have the same gray level. If the image is reduced to 64 gray levels, the trabeculae then appear in the same gray level range, and thus have change to form a run. So the original 16 bit CT images were quantized into 64 gray levels using linear mapping. From the gray level run length matrix features such as GLNU, RLNU, RP etc are calculated and stored as feature vector F1. From the histogram of the sub image energy,entropy,mean intensity etc were calculated and stored as feature vector F2.The discrete curvelet transform is a discretization of their continuous Curvelet Transform [9,11], which uses a "wrapping" algorithm. The transform consists of four steps: application of a 2-dimensional Fast Fourier transform of the image, formation of a product of scale and angle windows, wrapping this product around the origin, and application of a 2-dimensional inverse Fast Fourier transform. The approximate scales and orientation are supported by a generic 'wedge'. The discrete curvelet transform can be calculated to various resolutions or scales and angles. Two parameters are involved in the digital implementation of the curvelet transform: number of resolutions and number of angles at the coarsest level. For our images of 32x32, maximum resolution extraction was three levels of resolution, and 16 angles were found to be ideal. Several features were then calculated on the curvelet coefficients. Features such as mean and standard deviation are calculated from each of coarse level curvelet sub-bands and are stored in the data base. Co-occurrence matrix (C) is formed for each sub-band of DCvT, which gives the information about the spatial distribution of gray scale values. From the Co-occurrence matrix, the features such as contrast, sum-mean, cluster shade, cluster prominence and local homogeneity etc are calculated [14, 16, 17] and are stored in the feature data base. Variable pairs with R2 values >0.5 were further compared using polynomial regression with a 95% significance level.

Texture classification

The classification step was carried out to test the predictive power of the histogram features, run length features and curvelet based statistical & co occurrence features to classify implant recipient sites based on type of the bone by using the classification and regression trees analysis (CART) [19,20]. This multivariate approach, an alternative to linear regression techniques, can be used to predict categorical (classification) or continuous (regression) out comes. Multivariate methods often afford an increase in power to correctly classify subjects over methods using single variables. The most relevant texture descriptors were found for each type of bone ,and based on those selected descriptors, a set of decision rules were generated. These sets of rules were then used for the classification of each recipient site. To evaluate the performance of each classifier specificity and sensitivity were

calculated from each of the misclassification matrices.

Results and Discussion

The discriminating powers of the feature vectors, the feature variations in male and female at various implant recipient sites and comparison of curvelet based descriptors with co-occurrence and run length based techniques is described in the following section. The mean and standard deviation for each of the texture parameters from the 50 bone images (26 Male, 24 Female) are presented in Table 2. The CT slice of mandible and maxilla was shown in Figure 4.

Figure 4: I. Axial CT slice (Maxilla), II. Edge based segmentation, III. Axial CT slice (Mandible).

Three possible changes in image texture were observed based on the parameters of Table 2: First, as de calcification progress there could be an even reduction of intensity along the profiles; that is, no textural change would be observed apart from a mean decrease in intensity. Another is uneven or patchy bone demineralization with an initially dramatic increase in texture roughness at points along each profile. Finally, there could be an uneven reduction in profile intensity but with a smoothing of the image texture. Examination of changes in a gray level statistic matrix during demineralization will help to clarify these findings. For a typical image profile, non zero matrix elements were dispersed along or near its main diagonal before decalcification indicating relatively similar gray level pairs at separation $\Delta x=2$. After decalcification, the spread of this

Table 2: Gender wise significant texture parameters with varying age group

Parameter	*Male Age (39±8.6)*	*Female Age (39±8.6)*	*Male Age (61±10)*	*Female Age (61±10)*
RMS	45±8	30±10	90±12	70±9
Energy	4.30±1.85	3.35±1.3	6.18±2.15	5.28±1.7
Entropy	0.045±0.050	0.028±0.040	0.029±0.050	0.025±0.03
SRE	0.164±0.050	0.236±0.030	0.19±0.02	0.1±0.008
LRE	230±60	200±70	205±20	110±20
GLN	5200±300	2400±200	2800±300	6200±400
RLN	600±35	780±140	690±50	1100±130
RP	2.8±1.2	1.6±0.3	1.75±0.13	2.81±0.2
Contrast	3.08±1.02	2.06±0.5	2.2±0.05	3.2±0.7
Sum-Mean	7.3±2.0	5.5±0.4	5.2±0.7	5.8±0.30
Cluster-shade	3.01±1.1	2.05±0.5	3.0±1.2	3.2±0.7

distribution decreased dramatically, results of the profile texture becoming less irregular, changes in features such as angular second moment and entropy that are sensitive to this spread reflect this change. From the data angular second moment increased from 0.009 – 0.17 and entropy decreased from 4.64 to 2.67.The complete decalcification leads asm=1 and entropy= 0.

significant with $p<0.004$ among male and female patients showing the evidence of notable alterations of the trabecular architecture in addition to bone mineral density. It was found that the bone density in all patients ranged from 199-1109 HU. Bone density values based on the Hounsfield scale ranged from 51 to 529 in the mandible and 186-389 in the maxilla; anterior sites being higher in both.

Table 3: Bone quality classification vs. measure of cancellous bone density in HU for all sites

Site	*Bone quality classification*	*HU units (min-max)*
Anterior Mandible	2	529 (97-1109)
Right post Mandible	3	169 (-23-694)
Left post Mandible	3	101 (-11-356)
Anterior Maxilla	3	389 (101-825)
Right post Maxilla	4	186 (27-444)
Left post Maxilla	4	222 (102-367)

The contrast measure provides evidence of how sharp the structural variations in the image are. The angular second moment gives a strong measure of uniformity and higher non uniformity values provide evidence of higher structural variations. In females straight line series (runs) of pixels of similar gray levels significantly more frequent in lower alveolar ridge than upper alveolar ridge. Image brightness shows the highest correlation to CT ($r=0.97$, $p< 0.005$). This can be explained by the fact that lower calcium contents results in lower attenuation of X rays in the bone. By measuring changes in texture parameters it is possible to monitor changes in calcium contents and internal structure of the bone. Despite the fact that of the sites examined, bone density decreased by about 40% with age. Healthy aging men appear to lose bone by mechanisms different from those that cause age related bone loss in women. The RMS graph shows that when there is a significant decrease in bone mineral content the RMS values are increased. Out of twenty nine texture measures derived from histogram, run length matrix, curvelet based co occurrence matrix ten parameters and the RMS value of the power spectral density are found to be statistically

When each gray level in the ROI is equally probably, the resulting histogram is uniform. Entropy takes on a maximal value and energy a minimal value. As mineral was lost, the distribution of pixel intensities shifted and became relatively more concentrated in the lower gray levels, entropy concomitantly decreased and energy increased. Theoretically, an entire histogram distribution could shift to the left intact with a decrease in μI. Correlation analysis revealed a strong linear association between percentage maxillary alveolar calcium loss and changes in μI. Consistent level of association was found between calcium loss and entropy ($r>0.95$) and a moderate level of association between calcium loss and energy ($r>0.65$). Mean intensity level decreased and the ruggedness of the intensity surface was smoothed. These pattern changes resemble radio graphic texture differences between younger and older women. The bone density in terms of Hounsfield units and the mean values of run length, curvelet based histogram features and co occurrence features were compared using student's t-test for male and female patients.

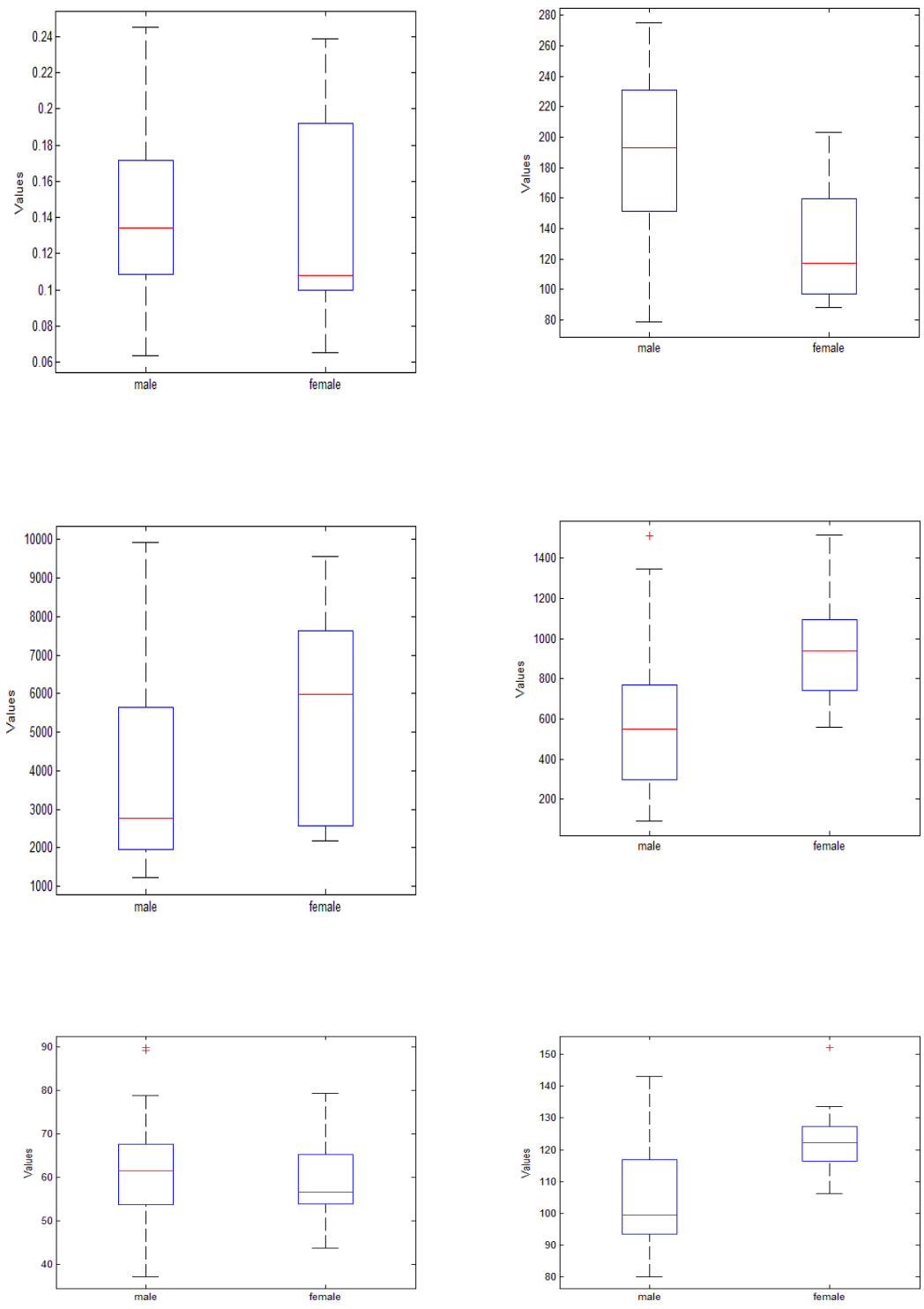

Fig5: (a) 95%CL SRE versus AGE, (b) 95%CL LRE versus AGE, (c) 95%CL GLN versus AGE, (d) 95%CL RLN versus AGE, (e) 95%CL MEAN versus AGE, (f) 95%CL CLUSTERTEN versus AGE

A visual representation of these values with 95% confidence intervals is shown in Figure 5 and the polynomial regressions are shown in Figure 6.

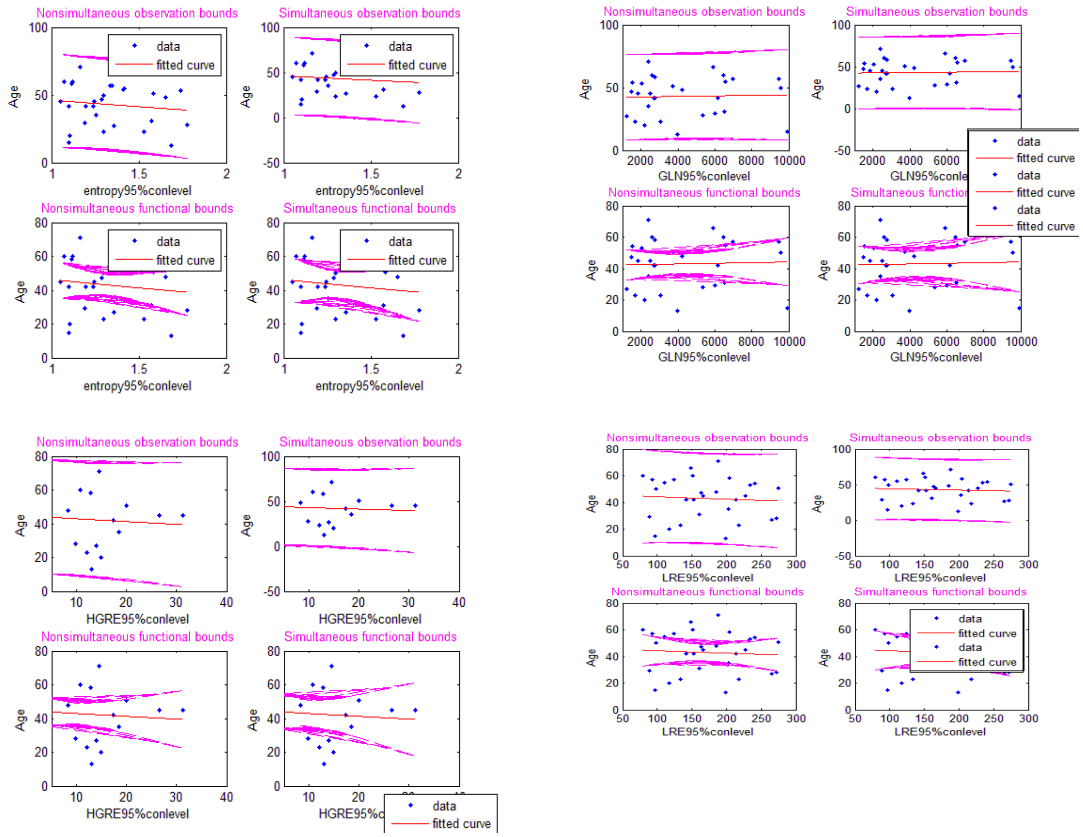

Fig6: (a-f) Polynomial regression graphs

Table 4 shows a comparison of the performance of five feature vectors using CART approach. The overall classification accuracy result achieved was 95.2 % (specificity 90.11%, sensitivity 92.13%) using the leave-one-out strategy due to small number of data samples. The sensitivity performance was in the 61%-91% range, with curvelet based features (F5) outperforming the others. Specificity performance was in the 72%-92% range with feature vector F5 outperforming others. Features from the Histogram and GLRL produced classification accuracy results above the threshold set. Features from the curvelet sub bands obtained by all the domains produced the best classification result, since they focus on the overall nature of the texture, complexity and gray tone transitions.

Table 4: Classification performance for all the feature vectors

Classifier	***Descriptors***	***Sensitivity***	***Specificity***	***PPV***	***NPV***	***Accuracy***
CART (with Leave-one-out method)	F1	61.52	72.28	78.26	58.52	87.8
	F2	65	77.6	80.4	61.87	90.24
	F3	67.2	77.78	89.13	73.5	91.1
	F4	85	89.5	71.2	65.3	92.89
	F5	90.11	92.13	82.56	73.8	95.2

**Data are expressed as percentage.* PPV- *positive predictive value;* NPV- *negative predictive value.*

Conclusion

Image data sets were obtained from 50 patients to obtain the bone quality in Hounsfield units at the implant recipient sites and texture parameters respectively.

The texture parameters derived by the run-length matrix, curvelet based statistical and co occurrence features on jaw bone CT images constitute a computer based assessment of bone quality. The minimal generalized calcium loss detected by these features is still a substantial improvement over the estimated 30-60% decalcification that must exist before a radiologist is certain of bone loss using conventional radio graphic interpretation. Bone in the maxilla should be loss concurrently with or even earlier than other axial bone. Texture features extracted based on curvelet transform and distribution of these features in various directions assist in characterizing alveolar bone. In this study ten out of twenty four texture parameters could predict changes in trabecular network. The alterations in the trabecular network with respect to advancing age were also quantified by the texture analysis. This noninvasive analysis may provide information about the trabecular architecture that is independent of bone mineral density but depends on age. One can conclude that by measuring changes in statistical texture parameters it is possible to monitor changes in calcium contents and internal structure of the bone. The results of this study indicate that curvelet based texture analysis is an effective tool that could quantify bone architecture as well as bone density in two dimensional bone slices. The major advantage of using a multi- resolution approach in this application is that it examines the directionality of the texture components at all scales (resolutions) simultaneously and independently. This method can be used by the implant surgeons to know about the bone quality at the implant sites pre operatively which can avoid the cost and trauma undergo by the patients.

Acknowledgement

The authors wish to express appreciation to the staff of Bharat Scans & Department of Radialogy, Raja Rajeswari Dental College for their help in clinical data collection.

References

1. Lekholm O, Zarb G A, Patient selection and preparation in Brane mark PI, Zarb G A Albertson T (Eds) Osseo integration in clinical dentistry, Quintessence, 1985; 199-209.

2. Yongqing Xiang, Vanessa R. Yingling. Comparative assessment of bone mass and structure using texture-based and histomorphometric analysis. Bone, 2007; 40: 544-552.

3. Andre Gahleitner, G.Watzek, H.Imhof. Dental CT: Imaging Technique, anatomy, and pathologic conditions of the jaws. Euro Radio, 2003; 23:366-376.

4. Teo J.C.M. Correlation of cancellous bone micro architectural parameters from microCT to CT number and bone mechanical properties. Materials science and Engineering, 2007; 27: 333-339.

5. Arivazhagan S and Ganesan L.Texture classification using wavelet transform. Pattern recognition Letters, 2003; 1513-1521.

6. Kara B & Watsuji N.Using Wavelets for Texture Classification. IJCI Proceedings of International Conference on Signal Processing, 2003; 1304-2386.

7. Do M.N & Vetterli M. The Finite Ridgelet Transform for Image Representation,.IEEE Transactions on Image Processing,2003;12: 16 - 28.

8. Candes E.J, Demanet L, Donoho D.L, Ying L. Fast Discrete Curvelet Transforms Technical Report, California Institute of Technology, 2005.

9. Ying L. CurvelLab 2.0. California Institute of Technology, 2005.

10. Donoho D.L and Duncan M.R. Digital Curvelet Transforms strategy, implementation and experiments. In proc Aero sense 2000, wavelet application VII, SPIE 2000; vol-4056: pp 12-29.

11. Candes E.J, Donoho D.L. New tight frames of curvelets and optimal representation of objects with C2 singularities.Comm pure appl math, 2004; Vol.57, No.2: pp-219-266.

12. Candes E. J. & Donoho D. L. Curvelets, Multi-resolution Representation, and Scaling Laws. Wavelet Applications in Signal and Image Processing VIII, 2000; SPIE 4119.

13. Kurani A, D.H. Xu, J.D. Furst, D.S. Raicu. Co occurrence matrices for volumetric Data. The 7th IASTED International Conference on Computer Graphics and Imaging CGIM 2004, Hawaii, USA.

14. Xu D.H, A.Kurani. Run-length encoding for volumetric texture. VIIP 2004.

15. Haralick R.M., Shanmugam K, Dinstein I. Texture features for image classification. IEEE Transactions on System Man Cybernat, 1973; Vol, 8, No. 6: pp. 610-621.

16. Semler L & Dettori L.A Comparison of Wavelet-Based and Ridgelet-Based Texture Classification of Tissues in Computed Tomography. Proceedings of International Conference on Computer Vision Theory and Applications, 2006.

17. Ulrich D, Van Reitbergen B, Laib A, Ruegsegger P.The ability of three-dimensional Structural indices to reflect mechanical aspects of trabecular bone.Bone,1995;25 (1):55- 60.

18. Fukunaga K.Introduction to statistical pattern recognition. IInd edition, Academic Press, San DiegoCA, USA, 1990.

19. Kornel, P., Bela, M., Rainer, S., Zalan, D., Zsolt, T. and Janos, F. Application of neural network in medicine". Diag. Med. Tech., 1998; 4 (3): 538-546